

Magnetic response of the $J_1 - J_2$ spin Hamiltonian from classical Monte Carlo and Schwinger boson mean field theory

Zhihua Yang,¹ Jung Hoon Kim,² and Jung Hoon Han^{2,*}

¹*Institute of Basic Science, Sungkyunkwan University, Suwon 440-746, Korea*

²*Department of Physics, BK21 Physics Research Division,
Sungkyunkwan University, Suwon 440-746, Korea*

(Dated: November 20, 2018)

Magnetic susceptibilities at several potential ordering wave vectors $(0,0)$, $(\pi,0)$, and (π,π) are analyzed for the antiferromagnetic $J_1 - J_2$ spin Hamiltonian by classical Monte Carlo and Schwinger boson mean field theories over the parameter range $0 \leq 2J_2/J_1 \leq 2$. We find a nearly linear- T behavior of the uniform susceptibility that extends up to the temperature scale of J_1 within both calculation schemes when $2J_2/J_1$ is sufficiently removed from the critical point $2J_2/J_1 = 1$. The window of linear temperature dependence diminishes as the critical point is approached.

PACS numbers: 74.25.Ha, 71.27.+a, 75.30.Fv

I. INTRODUCTION

One of the outstanding issues for the spin density wave (SDW) phase of the parent FeAs compound is whether a localized spin model can be justifiably used for the description of spin dynamics. The concern arises mainly from the fact that, unlike the parent compound of cuprate high-temperature superconductors, the parent material for FeAs-based superconductors is metallic and the validity of the description which ignores the itinerant electrons is not nearly as water-tight as with the half-filled cuprate compound. Despite these concerns, the $J_1 - J_2$ spin model had been proposed for the spin dynamics of the FeAs parent compound^{1,2} which, disregarding the multi-orbital character of the FeAs band structure, reads

$$H_S = J_1 \sum_{\langle ij \rangle} \mathbf{S}_i \cdot \mathbf{S}_j + J_2 \sum_{\langle ik \rangle} \mathbf{S}_i \cdot \mathbf{S}_k. \quad (1)$$

The nearest neighbor (NN) and next-nearest neighbor (NNN) pairs are written as $\langle ij \rangle$ and $\langle ik \rangle$, respectively. From first-principles calculations one obtains the estimate $J_1 \sim J_2$ and J_1 in the range of several hundred Kelvin^{2,3}.

Of particular relevance in connection with the magnetic response of FeAs is the behavior of the uniform susceptibility χ_u . The temperature dependence of χ_u was found to be linear up to 500-700K⁴, well beyond the SDW ordering temperature $T_{\text{SDW}} \sim 150\text{K}$. The relevance of the $J_1 - J_2$ spin Hamiltonian to the FeAs phenomenology largely depends on its ability to reproduce the observed temperature dependence of χ_u . The uniform susceptibility for the J_1 -only model has been calculated semi-classically by Takahashi⁵ and more recently by classical Monte Carlo (MC) calculations⁶, demonstrating a roughly linear behavior of $\chi_u(T)$ in the low-temperature regime below the mean-field transition temperature, T_{MF} . The quantum spin-1/2 Heisenberg Hamiltonian was also found to have a low-temperature

region with a roughly linear temperature-dependent χ_u ⁷.

A recent note by Zhang *et al.*⁸ cites such susceptibility behavior as evidence of pre-formed moments in FeAs in the paramagnetic regime. A quasi-linear temperature dependence of χ_u in the $J_1 - J_2$ spin Hamiltonian was demonstrated in a spin-wave calculation based on the Dyson-Maleev transformation of the spin operators⁸. A similar temperature dependence of the susceptibility was also found in a model based on the nonlinear sigma model description of the spin dynamics⁹. Both ideas^{8,9} support, and are based on the presence of pre-formed magnetic moments in the paramagnetic phase^{1,2}. In contrast to the Curie-Weiss susceptibility behavior of a local moment, the linear- T susceptibility is a reflection of the non-trivial correlation among the moments in the paramagnetic state, and a deeper understanding of the magnetic response in such a correlated paramagnetic phase is highly desirable.

A lot is known about the classical $J_1 - J_2$ model from previous theoretical works^{10,11}. Although no true long-range order is possible in two dimensions, the mean-field ground state is antiferromagnetically ordered at the wave vector $k = (\pi, \pi)$ when $2J_2/J_1 < 1$. For $2J_2/J_1 > 1$, the two sublattices separately support a mean-field staggered magnetic phase while the relative orientation of the sublattice magnetization vectors remains undetermined. It is the thermal fluctuations which selects a collinear spin order at $k = (\pi, 0)$ or $k = (0, \pi)$ through an order-by-disorder mechanism¹⁰. A quantum spin-1/2 version of the $J_1 - J_2$ has recently received some theoretical attention¹², but the relevant uniform magnetic susceptibility χ_u has not been calculated in the quantum model.

In this paper, we re-visit the susceptibility behavior of the $J_1 - J_2$ spin model in a comprehensive and unified fashion using both classical Monte Carlo (MC) methods and the Schwinger boson mean field theory (SBMFT). Previous analytic and numerical works^{5-8,12} typically have examined the susceptibility for a particular ordering wave vector. In the $J_1 - J_2$ spin model the dominant ordering

wave vector switches from (π, π) for $2J_2/J_1 < 1$ to $(\pi, 0)$ for $2J_2/J_1 > 1$. The fate of the non-dominant susceptibilities, for instance the susceptibility at $k = (\pi, 0)$ for the $2J_2/J_1 < 1$ region, has not been addressed carefully. The uniform susceptibility χ_u is not expected to be dominant for any $2J_2/J_1$ ratio, but its behavior has not been understood in a systematic way, either.

At the moment the controversy surrounding the itinerant¹³ vs. localized moment origin^{8,9} of the linear- T susceptibility is an on-going issue. A careful and systematic examination of the magnetic response of the $J_1 - J_2$ spin model by employing well-established techniques is expected to be a helpful addition to our knowledge required to settle the issue in the long run. The organization of the paper is as follows. In Sec. II, Monte Carlo calculation of the magnetic susceptibilities at several wave vectors are presented for all $2J_2/J_1$ ratios between 0 and 2, which encompasses the Heisenberg limit $2J_2/J_1 = 0$ and the critical point at $2J_2/J_1 = 1$. And in Sec. III a Schwinger boson mean-field calculation employing several order parameters which embody both (π, π) and $(\pi, 0)$ ordering are presented over the same $2J_2/J_1$ range. We conclude with a discussion in Sec. IV. The properties of the uniform and (π, π) -staggered magnetic susceptibilities of the J_1 -only Hamiltonian in the SBMFT are reviewed in the Appendix.

II. MONTE CARLO EVALUATION OF THE MAGNETIC SUSCEPTIBILITY

Classical mean field analysis of the $J_1 - J_2$ model assuming the ordering pattern $\langle S_i \rangle = m_1(-1)^{x_i} + m_2(-1)^{x_i+y_i}$ (coexistence of $(\pi, 0)$ and (π, π) order) is reduced to the coupled set of mean-field equations

$$\begin{aligned} m_1 + m_2 &= \tanh\left(\frac{2}{T}[(J_2 m_1 + (J_1 - J_2)m_2)]\right), \\ m_1 - m_2 &= \tanh\left(\frac{2}{T}[J_2 m_1 - (J_1 - J_2)m_2]\right). \end{aligned} \quad (2)$$

As shown in Fig. 1, either a (π, π) -ordered phase ($m_1 = 0, m_2 \neq 0$) or a $(\pi, 0)$ -ordered phase ($m_1 \neq 0, m_2 = 0$) is favored depending on the $2J_2/J_1$ value being less or greater than one. No co-existence region exists where m_1 and m_2 are simultaneously nonzero. A first-order line separates the two phases at $2J_2/J_1 = 1$. In the Ginzburg-Landau picture, a repulsive interaction $v|m_1|^2|m_2|^2$ term with $v > 0$ exists between the order parameters.

With this classical mean field phase diagram in mind, we have measured the magnetic susceptibilities at three wave vector positions, $k = (0, 0)$, $(\pi, 0)$, and (π, π) , for the range $0 \leq 2J_2/J_1 \leq 2$ that also encompasses the critical point $2J_2/J_1 = 1$. For a given k vector, the susceptibility χ_k^α for the component $\alpha = x, y, z$ is computed according to

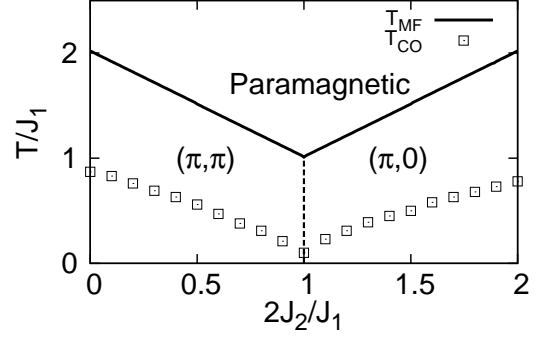


FIG. 1: Mean-field phase diagram of the $J_1 - J_2$ classical spin model. (π, π) -ordered phase is separated by a first-order line (dotted) at $2J_2/J_1 = 1$ from the $(\pi, 0)$ -ordered phase. Crossover temperature T_{CO} extracted from the uniform susceptibility in the classical Monte Carlo calculation is shown for comparison.

$$\langle S_k^\alpha \rangle = \sum_i \langle S_i^\alpha \rangle e^{-ik \cdot r_i}, \quad \chi_k^\alpha = \frac{\langle S_{-k}^\alpha S_k^\alpha \rangle - \langle S_{-k}^\alpha \rangle \langle S_k^\alpha \rangle}{TN}. \quad (3)$$

Here N stands for the number of lattice sites, and $\langle \dots \rangle$ is the thermal average.

In agreement with the mean-field analysis, the (π, π) susceptibility rises sharply at a finite temperature T_c in the region $2J_2/J_1 < 1$. For the $(\pi, 0)$ susceptibility the sharp rise occurs on the $2J_2/J_1 > 1$ side. At $2J_2/J_1 = 1$ both susceptibilities showed increasing behavior at lower temperatures. This temperature T_c however decreases when a larger lattice size is used in the simulation, in accordance with the Mermin-Wagner theorem which prohibits long-range order in a continuous spin model. We will not discuss the behavior of the dominant susceptibilities any further and turn our attention to non-dominant susceptibilities.

Results of the MC calculation for the non-divergent susceptibilities are shown in Fig. 2. The uniform susceptibility $\chi_{(0,0)}$, which remains non-divergent for all values of $2J_2/J_1$, does show the low-temperature linear- T behavior up to a certain crossover temperature scale, T_{CO} ¹⁴. Furthermore, T_{CO} grows as the $2J_2 - J_1$ value moves away from criticality. The crossover temperature T_{CO} can be extracted from the $\chi_{(0,0)}$ data due to the fairly abrupt deviation from low-temperature linearity at $T \approx T_{CO}$. A plot of T_{CO} over the range $0 \leq 2J_2/J_1 \leq 2$ is shown in Fig. 1 along with the mean-field transition temperature T_{MF} . Due to the thermal fluctuation effects, T_{CO} remains substantially smaller than the corresponding T_{MF} . Even at the critical point $2J_2/J_1 = 1$ the crossover scale remains finite at $T_{CO}/J_1 \sim 0.1$.

The behavior of non-divergent $\chi_{(\pi,0)}$ for $2J_2/J_1 < 1$, and $\chi_{(\pi,\pi)}$ for $2J_2/J_1 > 1$ are also shown in Fig. 2. Interestingly, these susceptibilities also show a linear temperature dependence at low temperatures, and find the

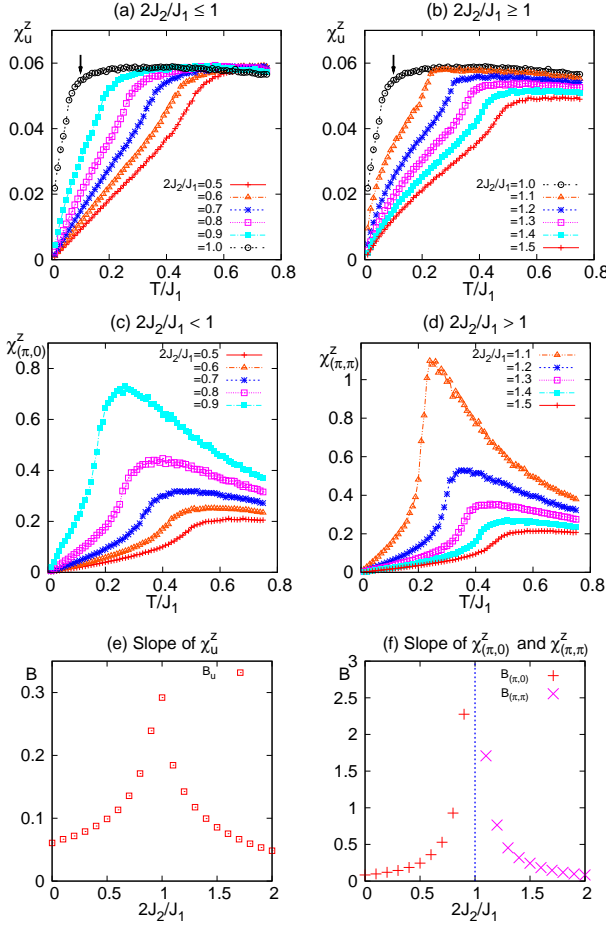


FIG. 2: (color online) Temperature dependence of (a) uniform susceptibility $\chi_{(0,0)}^z$ for $2J_2/J_1 \leq 1$, (b) $\chi_{(0,0)}^z$ for $2J_2/J_1 \geq 1$, (c) staggered susceptibility $\chi_{(\pi,0)}^z$ for $2J_2/J_1 < 1$, and (d) staggered susceptibility $\chi_{(\pi,\pi)}^z$ for $2J_2/J_1 > 1$. Data are obtained for a 16×16 lattice with 5×10^5 MC steps per data point. Several calculations run on a 40×40 lattice gave virtually identical curves as those of a 16×16 lattice over the whole temperature interval. The crossover temperature such as indicated by an arrow in (a) and (b) marks the deviation from low-temperature linearity. We have plotted the z -component of the susceptibilities for an easier determination of T_{CO} ¹⁴. (e) Slopes of the low-temperature linear part of $\chi_{(0,0)}^z$ vs. T/J_1 . (f) Slopes of the low-temperature linear part of $\chi_{(\pi,0)}^z$ for $2J_2/J_1 < 1$ and $\chi_{(\pi,\pi)}^z$ for $2J_2/J_1 > 1$. Both slopes become sharper near the critical point.

maximum value at $T \approx T_{CO}$. Unlike the uniform susceptibility, these two quantities exhibit divergent behavior right at the critical point $2J_2/J_1 = 1$, and are omitted from the plot in Fig. 2. In terms of absolute scale, the $(\pi, 0)$ and (π, π) susceptibilities are about an order of magnitude bigger than χ_u . The linearity can be characterized by fitting the low-temperature part with the form $\chi^z = B(T/J_1)$. The slope B of the linear parts of the susceptibilities are shown in Fig. 2(e) for the uniform part and Fig. 2 for the staggered parts.

Based on the results of MC calculations, we conclude that the linear- T behavior of the uniform susceptibility is a natural aspect of the $J_1 - J_2$ spin model for the $2J_2/J_1$ ratio that spans both sides of the critical point, and presumably for a wider class of spin models whose mean-field ordering wave vector occurs well away from $(0, 0)$. In fact, the linearity of $\chi_u(T)$ persists over a wider temperature range when $2J_2/J_1$ departs further from the critical value. If we take the estimate $J_1 = J_2 = 500K^2$, the expected crossover temperature from the MC calculation is $T_{CO} \sim 0.8J_1 \sim 400K$, in fair proximity to the 500-700 K up to which the linear susceptibility has been observed. It is also clear that the linear- T susceptibility behavior alone does not imply the proximity of the FeAs system to a critical point nor the existence of high degree of spin frustration.

III. SCHWINGER BOSON MEAN FIELD THEORY OF THE MAGNETIC SUSCEPTIBILITY

The quantum analogue of the classical susceptibilities can be obtained by treating the $J_1 - J_2$ spin Hamiltonian in the framework of Schwinger boson mean field theory (SBMFT). A prior calculation⁸ assumed an ordering wave vector $K_x = (\pi, 0)$, or equivalently at $K_y = (0, \pi)$, and ignored the possibility of ordering at $Q = (\pi, \pi)$. While this assumption may be sound deep in the J_2 -dominated part of the phase diagram, here we want to make an unbiased statement that spans both small and large $2J_2/J_1$ regions and keep both $(\pi, 0)$ and (π, π) order parameters in the theory. The details of the self-consistent Schwinger boson calculation for the J_1 -only spin model can be found in the work of Auerbach and Arovas¹⁵.

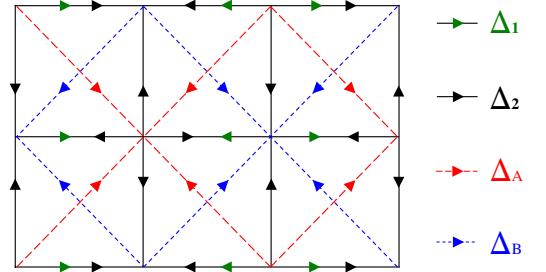


FIG. 3: (color online) Schematic picture of the pairing amplitudes Δ_{ij} used in our calculation. The values of Δ_{ij} for the arrows going from site i to site j are indicated on the right. Note that $\Delta_{ji} = -\Delta_{ij}$.

For SBMFT calculations one first re-writes the $J_1 - J_2$ Hamiltonian in the mean-field form

$$H_{MF} = -\frac{J_1}{2} \sum_{\langle ij \rangle} \Delta_{ij}^* A_{ij} - \frac{J_2}{2} \sum_{\langle ik \rangle} \Delta_{ik}^* A_{ik} + h.c. \\ + \sum_i \lambda_i (b_{i1}^\dagger b_{i1} + b_{i2}^\dagger b_{i2} - 2S), \quad (4)$$

where the operators are $A_{ij} = b_{i1}b_{j2} - b_{i2}b_{j1} = -A_{ji}$, and $\Delta_{ij} = \langle A_{ij} \rangle$. The b_{i1} and b_{i2} are the two species of boson operators that obey the occupation constraint $b_{i1}^\dagger b_{i1} + b_{i2}^\dagger b_{i2} = 2S$, which is enforced with the Lagrange multiplier λ_i .

The distribution of Δ_{ij} adopted in our calculation is schematically shown in Fig. 3. The nearest-neighbor pairing fields are assumed to be modulated at both K_x and Q with the respective amplitudes Δ_1 and Δ_2 :

$$\Delta_{i,i\pm\hat{x}} = \Delta_2(-1)^{x_i+y_i} + \Delta_{1x}(-1)^{x_i}, \\ \Delta_{i,i\pm\hat{y}} = \Delta_2(-1)^{x_i+y_i} + \Delta_{1y}(-1)^{x_i}. \quad (5)$$

By symmetry, it turns out, Δ_{1y} vanishes identically and we can re-write $\Delta_{1x} = \Delta_1$. For the assumed ordering at $(0, \pi)$ we would have $\Delta_{1x} = 0$ instead. Without loss of generality we choose to work with the $(\pi, 0)$ modulation below. As for the interactions among the next-nearest neighbors let us write

$$\Delta_{i,i\pm\hat{x}\pm\hat{y}} = \frac{\Delta_A + \Delta_B}{2}(-1)^{y_i} + \frac{\Delta_A - \Delta_B}{2}(-1)^{x_i}. \quad (6)$$

It will be shown that $\Delta_A = \Delta_B$ whenever they are nonzero.

Due to the enlarged unit cell in real space assumed by the ordering pattern, the Brillouin zone is reduced to $[-\frac{\pi}{2}, \frac{\pi}{2}] \times [-\frac{\pi}{2}, \frac{\pi}{2}]$, and the Hamiltonian is expressed with an 8-component spinor

$$\psi_k = \begin{pmatrix} b_{k1} \\ b_{k+K_x1} \\ b_{k+K_y1} \\ b_{k+Q1} \\ b_{k2}^\dagger \\ b_{k+K_x2}^\dagger \\ b_{k+K_y2}^\dagger \\ b_{k+Q2}^\dagger \end{pmatrix}, \quad H = \sum_k \psi_k^\dagger \begin{pmatrix} \lambda & \mathcal{H}_k^+ \\ \mathcal{H}_k & \lambda \end{pmatrix} \psi_k. \quad (7)$$

The 4×4 matrix \mathcal{H}_k is given by

$$\begin{pmatrix} 0 & -\Delta_{1k} - \Delta_{3k} & -\Delta'_{3k} & -\Delta_{2k} \\ \Delta_{1k} + \Delta_{3k} & 0 & \Delta'_{2k} & \Delta'_{3k} \\ \Delta'_{3k} & -\Delta'_{2k} & 0 & -\Delta_{1k} + \Delta_{3k} \\ \Delta_{2k} & -\Delta_{3k} & \Delta_{1k} - \Delta_{3k} & 0 \end{pmatrix}, \quad (8)$$

where

$$\begin{aligned} \Delta_{1k} &= J_1 \Delta_1 \cos k_x, \\ \Delta_{2k} &= J_1 \Delta_2 (\cos k_x + \cos k_y), \\ \Delta'_{2k} &= J_1 \Delta_2 (\cos k_x - \cos k_y), \\ \Delta_{3k} &= J_2 (\Delta_A - \Delta_B) \cos k_x \cos k_y, \\ \Delta'_{3k} &= J_2 (\Delta_A + \Delta_B) \cos k_x \cos k_y. \end{aligned} \quad (9)$$

Note the antisymmetry $(\mathcal{H}_k)_{\mu\nu} = -(\mathcal{H}_k)_{\nu\mu}$. The sum \sum'_k extends over the reduced Brillouin zone (RBZ) only. The four kinds of momentum “flavors” $(k, k + K_x, k + K_y, k + Q)$ can be organized with an index $\alpha = 1 \sim 4$: $(b_{k\sigma}, b_{k+K_x\sigma}, b_{k+K_y\sigma}, b_{k+Q\sigma}) \rightarrow (b_{k,1\sigma}, b_{k,2\sigma}, b_{k,3\sigma}, b_{k,4\sigma})$. Rotation to the eigenoperators are implemented through

$$b_{k,\alpha 1} = \sum_{a=1}^4 (u_{k,\alpha a} \gamma_{k,a1} + v_{k,\alpha a}^* \gamma_{k,a2}^+), \\ b_{k,\alpha 2} = \sum_{a=1}^4 (u_{k,\alpha a} \gamma_{k,a2} - v_{k,\alpha a}^* \gamma_{k,a1}^+), \quad (10)$$

which would yield

$$H = \sum_{k,a} E_{k,a} (\gamma_{k,a1}^+ \gamma_{k,a1} + \gamma_{k,a2}^+ \gamma_{k,a2}). \quad (11)$$

It is convenient to group the wave function components as $\mathbf{u}_{k,a} = (u_{k,1a}, u_{k,2a}, u_{k,3a}, u_{k,4a})^T$, and $\mathbf{v}_{k,a} = (v_{k,1a}, v_{k,2a}, v_{k,3a}, v_{k,4a})^T$, after which the equations of motion becomes

$$\begin{aligned} \lambda \mathbf{u}_{k,a} + \mathcal{H}_k^+ \mathbf{v}_{k,a} &= E_{k,a} \mathbf{u}_{k,a}, \\ \lambda \mathbf{v}_{k,a} + \mathcal{H}_k \mathbf{u}_{k,a} &= -E_{k,a} \mathbf{v}_{k,a}, \end{aligned} \quad (12)$$

or

$$\begin{aligned} (\lambda^2 - E_{k,a}^2) \mathbf{u}_{k,a} &= \mathcal{H}_k^+ \mathcal{H}_k \mathbf{u}_{k,a}, \\ (\lambda^2 - E_{k,a}^2) \mathbf{v}_{k,a} &= \mathcal{H}_k \mathcal{H}_k^+ \mathbf{v}_{k,a}. \end{aligned} \quad (13)$$

The matrix $\mathcal{M}_k = \mathcal{H}_k^+ \mathcal{H}_k = \mathcal{H}_k \mathcal{H}_k^+$ is Hermitian and all its eigenvalues are non-negative. It proved to be an enormous advantage to deal with the ordinary Hermitian matrix problem of Eq. (13) over a non-Hermitian one posed by Eq. (12). With the eigenvalues of \mathcal{M}_k written $m_{k,a}^2$, the energy spectrum is obtained as $E_{k,a} = \sqrt{\lambda^2 - m_{k,a}^2}$.

One can either solve for $\mathbf{u}_{k,a}$ or $\mathbf{v}_{k,a}$ from Eq. (13), and derive the other part using

$$\mathbf{v}_{k,a} = -\frac{\mathcal{H}_k \mathbf{u}_{k,a}}{E_{k,a} + \lambda} \quad \text{or} \quad \mathbf{u}_{k,a} = \frac{\mathcal{H}_k^+ \mathbf{v}_{k,a}}{E_{k,a} - \lambda}. \quad (14)$$

The normalization for $\mathbf{u}_{k,a}$ and $\mathbf{v}_{k,a}$ reads

$$\mathbf{u}_{k,a}^* \cdot \mathbf{u}_{k,b} = \frac{\lambda + E_{k,a}}{2E_{k,a}} \delta_{ab}, \quad \mathbf{v}_{k,a}^* \cdot \mathbf{v}_{k,b} = \frac{\lambda - E_{k,a}}{2E_{k,a}} \delta_{ab}, \quad (15)$$

to ensure $\mathbf{u}_{k,a}^* \cdot \mathbf{u}_{k,b} - \mathbf{v}_{k,a}^* \cdot \mathbf{v}_{k,b} = \delta_{ab}$.

The averages of the boson operators we need are

$$\langle b_{k,\alpha 1} b_{\bar{k},\beta 2} \rangle = \sum_{a=1}^4 \left(v_{k,\alpha a}^* u_{k,\beta a} B_{k,a} - u_{k,\alpha a} v_{k,\beta a}^* (1 + B_{k,a}) \right) \quad (16)$$

where $B_{k,a}$ is the Bose-Einstein function of energy $E_{k,a}$, and $\bar{k} = -k$. The order parameters introduced for the mean field calculation are

$$\begin{aligned} \Delta_1 &= -\frac{2}{N} \sum_k \cos k_x \langle b_{k1} b_{\bar{k}+K_x 2} \rangle \\ &= \frac{2}{N} \sum_{k,a} \cos k_x (u_{k,1a} v_{k,2a}^* - u_{k,2a} v_{k,1a}^* + u_{k,3a} v_{k,4a}^* - u_{k,4a} v_{k,3a}^*) \coth \left(\frac{\beta E_{k,a}}{2} \right), \\ \Delta_2 &= -\frac{1}{N} \sum_k (\cos k_x + \cos k_y) \langle b_{k1} b_{\bar{k}+Q_2} \rangle \\ &= \frac{1}{N} \sum_{k,a} [(\cos k_x + \cos k_y) (u_{k,1a} v_{k,4a}^* - u_{k,4a} v_{k,1a}^*) + (\cos k_x - \cos k_y) (u_{k,3a} v_{k,2a}^* - u_{k,2a} v_{k,3a}^*)] \coth \left(\frac{\beta E_{k,a}}{2} \right), \\ \Delta_A &= -\frac{2}{N} \sum_k \cos k_x \cos k_y \langle b_{k1} b_{\bar{k}+K_y 2} + b_{k1} b_{\bar{k}+K_x 2} \rangle \\ &= \frac{2}{N} \sum_{k,a} \cos k_x \cos k_y [(u_{k,1a} + u_{k,4a}) (v_{k,2a}^* + v_{k,3a}^*) - (u_{k,2a} + u_{k,3a}) (v_{k,1a}^* + v_{k,4a}^*)] \coth \left(\frac{\beta E_{k,a}}{2} \right), \\ \Delta_B &= \frac{2}{N} \sum_k \cos k_x \cos k_y \langle b_{k1} b_{\bar{k}+K_x 2} - b_{k1} b_{\bar{k}+K_y 2} \rangle \\ &= \frac{2}{N} \sum_{k,a} \cos k_x \cos k_y [(u_{k,2a} - u_{k,3a}) (v_{k,1a}^* - v_{k,4a}^*) - (u_{k,1a} - u_{k,4a}) (v_{k,2a}^* - v_{k,3a}^*)] \coth \left(\frac{\beta E_{k,a}}{2} \right), \\ 2S+1 &= \frac{1}{N} \sum_{k,a} \frac{\lambda}{E_{k,a}} \coth \left(\frac{\beta E_{k,a}}{2} \right). \end{aligned} \quad (17)$$

The last line reflects the boson occupation numbers satisfy $(1/N) \sum_k \langle b_{k,1}^\dagger b_{k,1} + b_{k,2}^\dagger b_{k,2} \rangle = 2S$.

We have considered two spin values, $S = 1/2$, and $S = 1$, in the self-consistent calculation. The low-temperature ($T/J_1 = 0.001$) behavior of the gap parameters are shown in Fig. 4 over the range $0 \leq 2J_2/J_1 \leq 2$. There are two regions showing distinct behaviors, separated at $2J_2/J_1 = \eta_c$, η_c is a spin-dependent critical point. For $S = 1/2$ the critical point is $\eta_c = 1.2$, but $\eta_c = 1.1$ when $S = 1$ ¹². We found that $\eta_c = 1$ as long as $S \geq 2$, which is in agreement with the classical result. In Figs. 4 (a) and (b), for $2J_2/J_1 < \eta_c$ one finds $\Delta_A = 0 = \Delta_B$, and $\Delta_1 \neq 0 \neq \Delta_2$, and $2J_2/J_1 > \eta_c$ gives

$\Delta_A = \Delta_B$ nonzero, but $\Delta_1 = 0$. On the other hand Δ_2 remains nonzero throughout the whole range, although its magnitude decreases with the onset of nonzero Δ_A .

A surprising feature of the SBMFT result that needs to be emphasized is that Δ_1 , representing $(\pi, 0)$ order for the NN bonds in the x -direction, becomes nonzero even at $2J_2/J_1 = 0$ and stays finite (constant, in fact) all through $2J_2/J_1 = \eta_c$. Their temperature dependence for $2J_2/J_1 < \eta_c$ is shown in Fig. 4 (c) and (d), which tell us that both gap parameters become non-zero at the same temperature. A spontaneous loss of rotational symmetry is implied by nonzero Δ_1 . As long as $\Delta_A = 0 = \Delta_B$ the $J_1 - J_2$ Hamiltonian in SBMFT is the same as the J_1 -only model, with no influence from the presence of the

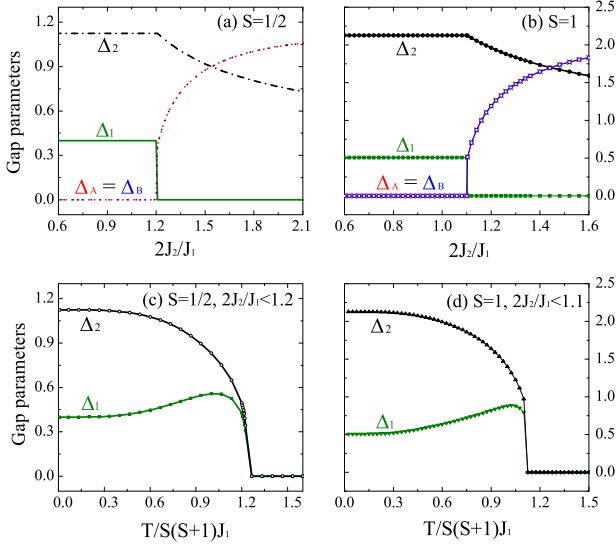


FIG. 4: (color online) Dependence of the gap parameters on the ratio $2J_2/J_1$ at low temperature, $T/J_1 = 0.001$ for (a) $S = 1/2$ and (b) $S = 1$. Temperature dependence of the gap parameters Δ_1 and Δ_2 when $2J_2/J_1 < \eta_c$ for (c) $S = 1/2$ and (d) $S = 1$. The temperature is divided by the exchange energy scale $J_1 S(S+1)$. The plot shows the onset of both Δ_1 and Δ_2 at the same temperature T_{MF}^{SBMFT} .

J_2 interaction. This explains the constancy of the gap parameters throughout $0 \leq 2J_2/J_1 < \eta_c$.

The equal-time magnetic susceptibility at wave vector k given in Eq. (3) can be calculated, where $\langle S_k \rangle = 0$ and thus

$$\chi_k = \frac{\langle S_k^- \cdot S_k \rangle}{TN} = \frac{3}{4TN} \sum_{i,j} \left(\langle S_i^+ S_j^- \rangle + \langle S_i^- S_j^+ \rangle \right) e^{ik \cdot (r_i - r_j)}. \quad (18)$$

The SU(2) invariance of the spin-spin correlation was assumed in eliminating the $\langle S_i^z S_j^z \rangle$ correlation from the above. The structure factor $S_k^+ = \sum_{i,j} \langle S_i^+ S_j^- \rangle e^{ik \cdot (r_i - r_j)}$ in SBMFT reads

$$S_k^+ = \sum_{k_1, k_2} \left(\langle b_{k_1,1}^\dagger b_{k_1-k,2} \rangle \langle b_{k_2,2}^\dagger b_{k_2+k,1} \rangle + \langle b_{k_1,1}^\dagger b_{k_2,2} \rangle \langle b_{k_1-k,2} b_{k_2+k,1} \rangle + \langle b_{k_1,1}^\dagger b_{k_2,1} \rangle \langle b_{k_1-k,2} b_{k_2-k,2} \rangle \right). \quad (19)$$

The first term on the right-hand side, corresponding to the spin flip process, is identically zero. The other structure factor $S_k^- = \sum_{i,j} \langle S_i^- S_j^+ \rangle e^{ik \cdot (r_i - r_j)}$ is obtained from $S_k^- = S_k^+$, and the magnetic susceptibility reads

$$\chi_k = \frac{1}{2TN} (S_k^+ + S_k^-). \quad (20)$$

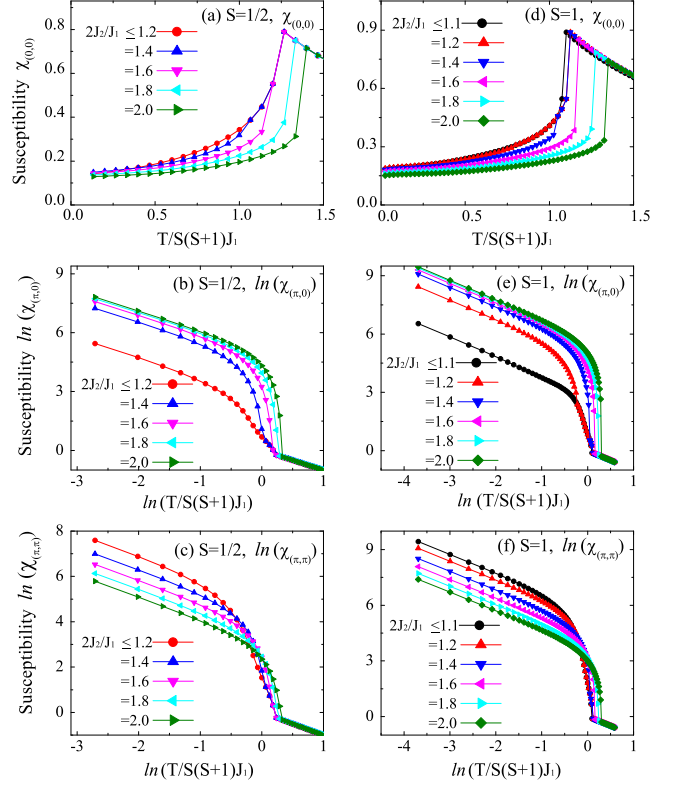


FIG. 5: (color online) Temperature dependence of the susceptibilities for several $2J_2/J_1$ ratios for $S = 1/2$ (left column) and $S = 1$ (right column). (a) and (d): $\chi_{(0,0)}$, (b) and (e) $\chi_{(\pi,0)}$. (c) and (f): $\chi_{(\pi,\pi)}$. $\chi_{(\pi,0)}$ and $\chi_{(\pi,\pi)}$ are shown on the log-log scale to emphasize the $1/T$ divergence at low temperature.

A factor $3/2$ has been divided out in arriving at Eq. (20) in order to obtain the correct high-temperature results¹⁵.

Three susceptibilities, $\chi_{(0,0)}$, $\chi_{(\pi,0)}$, and $\chi_{(\pi,\pi)}$, for spin $S = 1/2$ and $S = 1$, were calculated as shown in Fig. 5 for several $2J_2/J_1$ ratios. Above the mean-field transition temperature T_{MF}^{SBMFT} , all the gap parameters vanish identically and all the susceptibilities obey the Curie-Weiss form $\chi_k(T) = J_1 S(S+1)/T$ irrespective of k . Due to the constancy of the gap parameters for $2J_2/J_1 \leq \eta_c$ there are no variations in the susceptibility in this parameter range and it is sufficient to show only one susceptibility from this region in Fig. 5. We find T_{MF}^{SBMFT} depends on the spin S in the manner $T_{MF}^{SBMFT} \sim t J_1 S(S+1)$ where t is a $2J_2/J_1$ -dependent number. The staggered susceptibilities are plotted on a log-log scale in Fig. 5 to emphasize the $1/T$ divergence at low temperatures.

In the Appendix we show that the uniform susceptibility in the J_1 model follows the form $\chi_{(0,0)} = A + BT$ at low temperatures. Clearly the features of the uniform susceptibilities for all ranges of $2J_2/J_1$ are similar, with the main difference lying in the values of T_{MF}^{SBMFT} at which the collapse of the gap parameters occur and the susceptibility follows the Curie-Weiss form. The reduction in the slope B (defined in a loose sense as the

amount of increase divided by the temperature interval) with increasing $2J_2/J_1$ is found in both SBMFT and MC calculations. Although not nearly linear, the monotonic increase of the uniform susceptibility occurs over a larger temperature window when $2J_2/J_1$ is further removed from the critical point, in agreement with the earlier findings of Monte Carlo calculation.

The two staggered susceptibilities $\chi_{(\pi,0)}$ and $\chi_{(\pi,\pi)}$ show the temperature dependence which are qualitatively similar for all $2J_2/J_1$ ranges studied and thus bears strong resemblance to that of $\chi_{(\pi,\pi)}$ in the J_1 model. The properties of the latter quantity are discussed in the Appendix. Both susceptibilities diverge at low temperature as

$$\chi_{(\pi,0)} \sim \frac{N}{T}, \quad \text{and} \quad \chi_{(\pi,\pi)} \sim \frac{N}{T} \quad (21)$$

on both sides of the critical ratio η_c . The reason for the appearance of the factor N is explained in the Appendix as well. The reason for the simultaneous divergence of the two susceptibilities is the presence of Δ_1 for $2J_2/J_1 < \eta_c$ and $\Delta_{A(B)}$ for $2J_2/J_1 > \eta_c$, either of which would imply (quasi) ordering at $k = (\pi, 0)$. Due to the impossibility of long range ordering in two dimensions, the associated magnetic susceptibilities continue to diverge down to zero temperature. The scaling of the susceptibility with N is tied to the near Bose-Einstein condensation at low temperature (because true Bose-Einstein condensation cannot occur in two dimensions, either) as also discussed in the Appendix for the J_1 model. Finally, $\chi_{(0,\pi)}$ grows as $\sim 1/T$ without the factor N , and numerically much smaller than either $\chi_{(\pi,0)}$ or $\chi_{(\pi,\pi)}$.

The $(0, \pi)$ order, which has the corresponding gap parameter equal to zero, plays the role of the non-dominant susceptibilities in SBMFT. The Monte Carlo calculation in the previous section showed that such non-dominant susceptibilities, *i.e.* $\chi_{(\pi,0)}$ and $\chi_{(0,0)}$ for $2J_2/J_1 < 1$ and $\chi_{(\pi,\pi)}$ and $\chi_{(0,0)}$ for $2J_2/J_1 > 1$, are also non-divergent, going down to a constant value at zero temperature. Although $\chi_{(0,0)}$ behaves in the similar way in both treatments, $\chi_{(0,\pi)}$ behaves quite differently in SBMFT (diverging like $1/T$) as it does in classical theories (going down to a constant value). Even when a larger spin S is used in SBMFT, all three staggered susceptibilities diverge at low temperature and it is not obvious if the classical MC results can be fully recovered within the SBMFT. Regrettably, little is known in the literature about the connection of the SBMFT in the large- S limit to the classical results of the same Hamiltonian. While this would be an interesting issue in its own right, we leave it as a subject of future consideration.

The findings of the SBMFT study can be summarized as follows. The uniform susceptibility shows a monotonic temperature dependence that can be roughly understood as linearity. The mean-field transition temperature $T_{\text{MF}}^{\text{SBMFT}}$ plays a role similar to the crossover temperature T_{CO} in the classical theory, and has a larger value

when $2J_2/J_1$ gets larger (but only above the critical value η_c). Secondly, the two staggered susceptibilities $\chi_{(\pi,\pi)}$ and $\chi_{(\pi,0)}$ show the divergent behavior which is consistent with that of $\chi_{(\pi,\pi)}$ in the J_1 model. Both (π, π) and $(\pi, 0)$ (quasi) ordering are present in the SBMFT calculation for all ratios of $2J_2/J_1$ and only the relative weights of the corresponding susceptibilities shift with $2J_2/J_1$.

IV. SUMMARY AND DISCUSSION

In light of the recent controversy about how best to describe the spin dynamics of the parent FeAs compound above the magnetic ordering temperature, we carried out a detailed magnetic susceptibility calculation of the J_1 - J_2 spin Hamiltonian employing classical Monte Carlo and Schwinger boson mean field theory techniques over the parameter range $0 \leq 2J_2/J_1 \leq 2$. In both treatments the long-range magnetic ordering at finite temperature is absent and a thorough examination of the correlated paramagnetic phase becomes possible. In both approaches the uniform susceptibility was found to show a largely linear temperature dependence that extends up to the exchange energy scale $T \sim J_1$, in agreement with the persistence of linear susceptibility up to a few hundred Kelvin in FeAs compounds. Our calculation indicates that the linear- T uniform susceptibility behavior persists over a wider temperature range when $2J_2/J_1$ ratio is further removed from the critical point $2J_2/J_1 = 1$ (classical MC) or $2J_2/J_1 = \eta_c$ (SBMFT), and is largely independent of the degree of frustration in the spin model.

It was recently pointed out that the uniform susceptibility feature also exists in a model based on the itinerant electron picture¹³. To sharply test the validity of one model over the other for FeAs, then, one would have to go beyond the magnetic susceptibility issue to address other physical properties within both approaches. It is also desirable to generalize the J_1 - J_2 spin Hamiltonian to the doped case where the linear magnetic susceptibility was found to persist as well.

Acknowledgments

This work was supported by the Korea Science and Engineering Foundation (KOSEF) grant funded by the Korea government (MEST) (No. R01-2008-000-20586-0).

APPENDIX A: THE SUSCEPTIBILITY BEHAVIORS OF THE J_1 MODEL AT LOW TEMPERATURE

The antiferromagnetic Heisenberg model with $J_2 = 0$ and $J_1 = 1$ is

$$H_S = \sum_{\langle ij \rangle} \mathbf{S}_i \cdot \mathbf{S}_j, \quad (\text{A1})$$

has been studied in SBMFT by Auerbach and Arovas¹⁵, but it has not been analyzed in detail how the structure factors and the susceptibilities behave at low temperature for the finite system size $N = L \times L$. In this Appendix, we will give a simple explanation why the uniform and staggered susceptibilities behave as $\chi_{(0,0)} \sim A + BT$ and $\chi_{(\pi,\pi)} \sim N/T$ at low temperature in SBMFT for finite N .

The static structure factor is given by¹⁵

$$S_q^+ = \sum_k \left(\frac{\lambda^2 + \Delta_{2k} \Delta_{2k+q+Q}}{E_k E_{k+q+Q}} \left(B_k + \frac{1}{2} \right) \left(B_{k+q+Q} + \frac{1}{2} \right) - \frac{1}{4} \right), \quad (\text{A2})$$

where the definition of Δ_{2k} can be found in Eq. (9). The energy spectrum is $E_k = \sqrt{\lambda^2 - \Delta_{2k}^2}$, and the Bose-Einstein function is $B_k = 1/(e^{\beta E_k} - 1)$. The minimal value of E_k occurs at $k = (0,0)$ or $k = (\pi,\pi)$, and it is convenient to introduce the gap parameter $\delta \equiv \min(E_k) = \sqrt{\lambda^2 - 4\Delta_2^2}$. By numerical calculation we find at low temperature

$$\delta = C \frac{T^{1/2}}{L} \quad (\text{A3})$$

to an excellent fit and C is about 3.2 ($S = 1$).

For $q = (0,0)$, the uniform structure factor becomes

$$S_{(0,0)}^+ = \sum_k B_k (B_k + 1) = \frac{1}{4} \sum_k \frac{1}{\sinh^2(\beta E_k/2)}. \quad (\text{A4})$$

The energy spectrum expanded near $k = (0,0)$ and $k = (\pi,\pi)$ becomes $E_k \sim \sqrt{\delta^2 + \Delta_2^2 k^2}$. It is useful to separate

out the two points $k = (0,0)$ and $k = (\pi,\pi)$ from the above sum and treat the rest as an integral, which gives

$$\begin{aligned} S_{(0,0)}^+ &\sim \frac{1}{2 \sinh^2(\beta \delta/2)} + \frac{N}{4\pi} \int_{1/L}^{1/a} \frac{k dk}{\sinh^2(\beta \Delta_2 k/2)} \\ &\sim \frac{2T^2}{\delta^2} + \frac{NT^2}{\pi \Delta_2^2} \int_{1/L}^{1/a} \frac{dk}{k} \\ &\sim \frac{2NT}{C^2} + \frac{NT^2}{\pi \Delta_2^2} \ln \left(\frac{L}{a} \right), \end{aligned} \quad (\text{A5})$$

where $1/a$ serves as an upper momentum cutoff. Based on the relationship of the structure factor and the susceptibility in Eq. (18), one has

$$\chi_{(0,0)} \sim \frac{2}{C^2} + \frac{T}{\pi \Delta_2^2} \ln \left(\frac{L}{a} \right). \quad (\text{A6})$$

Indeed the low-temperature uniform susceptibility is given by the form $A + BT$.

For $q = (\pi,\pi)$, the structure factor becomes

$$S_{(\pi,\pi)}^+ = \sum_k \left(\frac{\lambda^2 + \Delta_{2k}^2}{\lambda^2 - \Delta_{2k}^2} \left(B_k + \frac{1}{2} \right)^2 - \frac{1}{4} \right). \quad (\text{A7})$$

The two isolated k -points $k = (0,0)$ and $k = (\pi,\pi)$ contribute to the structure factor

$$S_{(\pi,\pi)}^+ \sim \frac{4\lambda^2}{\delta^2} \times \frac{T^2}{\delta^2} \sim \frac{T^2}{\delta^4}, \quad (\text{A8})$$

when we approximate $(e^{\delta/T} - 1)^{-1} \approx T/\delta$. Inserting Eq. (A3) yields $S_{(\pi,\pi)} \sim N^2$ and hence the low-temperature susceptibility $\chi_{(\pi,\pi)} \sim N/T$. The contribution from the other k points is $S_{(\pi,\pi)}^+ \sim O(N)$.

* Electronic address: hanjh@skku.edu

¹ Qimiao Si and Elihu Abrahams, Phys. Rev. Lett. **101**, 076401 (2008).

² F. Ma, Z. Y. Lu, and T. Xiang, Phys. Rev. B **78**, 224517 (2008).

³ T. Yildirim, Phys. Rev. Lett. **101**, 057010 (2008).

⁴ G. Wu *et al.* J. Phys.: Condens. Matter **20**, 422201 (2008); J.-Q. Yan *et al.*, Phys. Rev. B **78**, 024516 (2008); X. F. Wang *et al.* arXiv:0806.2452; R. Klingeler *et al.* arXiv:0808.0708; X. F. Wang *et al.*, arxiv:0811.2920.

⁵ M. Takahashi, Phys. Rev. B **36**, 3791 (1987); **40**, 2494 (1989).

⁶ D. Hinzke, U. Nowak, and D. A. Garanin, Eur. Phys. J. B **16**, 435 (2000).

⁷ Miloje S. Makivić and Hong-Qiang Ding, Phys. Rev. B **43**,

3562 (1991); Jae-Kwon Kim and Matthias Troyer, Phys. Rev. Lett. **80**, 2705 (1998).

⁸ G. M. Zhang, Y. H. Su, Z. Y. Lu, Z. Y. Weng, D. H. Lee, and T. Xiang, arXiv:0809.3874v3.

⁹ Su-Peng Kou, Tao Li, and Zheng-Yu Weng, arXiv:0811.4111v3.

¹⁰ P. Chandra, P. Coleman, and A. I. Larkin, Phys. Rev. Lett. **64**, 88 (1990).

¹¹ Cédric Weber, Luca Capriotti, Grégoire Misguich, Federico Becca, Maged Elhajal, and Frédéric Mila, Phys. Rev. Lett. **91**, 177202 (2003).

¹² Luca Capriotti, Andrea Fubini, Tommaso Roscilde, and Valerio Tognetti, Phys. Rev. Lett. **92**, 157202 (2004).

¹³ M. M. Korshunov, I. Eremin, D. V. Efremov, D. L. Maslov, and A. V. Chubukov, arXiv:0901.0238v1.

¹⁴ The integration measure $\int d\theta \sin \theta$ in the partition function puts an extra factor $e^{\log(\sin \theta)}$ in the Metropolis ratio. As a result, the magnetic moments tend to order preferentially in the z -direction in the MC calculation. The magnetic susceptibilities also become direction-dependent. One can consider, as we have done, the averaged susceptibility $(\chi^x + \chi^y + \chi^z)/3$ after evaluating the susceptibility for each direction individually. Instead of showing the

direction-averaged susceptibilities, we present χ^z in Fig. 2 which shows a sharper turn and thus allows an easier determination of T_{CO} .

¹⁵ Assa Auerbach and Daniel P. Arovas, Phys. Rev. Lett. **61**, 617 (1988); Daniel P. Arovas and Assa Auerbach, Phys. Rev. B **38**, 316 (1988).